

FAST SIMULATION OF ULTRASOUND IMAGES FROM A CT VOLUME

S. Laguitton*, J.-J. Patard** and J.-L. Dillenseger*

* LTSI, INSERM, Univ. Rennes, 35042 Rennes, France

** Service d'Urologie, Hôpital de Pontchaillou, CHR Rennes, Rennes, France

jean-louis.dillenseger@univ-rennes1.fr

Abstract: The goal of our work is to propose a fast ultrasound images simulation from an abdominal CT volume. This method is based on a model elaborate by Bamber and Dickinson that predict the appearance and properties of a B-Scan ultrasound image from the distribution of point scatterers. However the main assumption of this method is that the US pulse and beam shape are assumed invariant. So this model can only be applied on small regions of interest. We propose to extend this model for abdominal ultrasound image simulation by taking into account the acoustical tissues properties and the geometry and the characteristics of the ultrasound probe (circular probe, transducers number and size, US pulse frequency and bandwidth, etc.). Simulations have been obtained in a fairly fast computation speed and qualitatively they present most of the real ultrasound images characteristics.

Introduction

For most of the surgical procedures the imaging techniques used to establish the preoperative planning are different to those used during the per-operative surgical treatment. This is the case for example, in urology and more particularly for a renal puncture. The preoperative planning is established on 3D images (CT, MRI) which provide high resolution anatomical information on the patient's case. In counterpart, the puncture is an ultrasound (US) image guided surgical act. Ultrasound is generally trickier to interpret. The connection between these both imaging techniques is problematic in terms of information correlation and interpretation (or moreover interpretation learning). A solution can be given by the simulation of ultrasound images from the preoperative 3D volumes and more specifically CT in our case.

Concerning the simulation of ultrasound scans, two main approaches have been previously proposed:

- The simulation and modeling of the emitted field, and the pulse-echo responses of the organs using linear acoustics. This is the case of Jensen's studies [1] where the organs are modeled using collections of point scatterers. The ultrasound image is estimated by the simultaneous study of the transducers interference, the physical, spatial and temporal ultrasound field propagation and its interaction with the scatterers. The precision of this approach is obtained to the

detriment of the computing time ¹.

- The direct prediction of the ultrasound images appearance from the single scatterers' contribution. The pioneer study has been proposed by Bamber and Dickinson [3]. It is based on the relation between the ultrasonic field/point scatterers' interaction and the final produced ultrasound image appearance. If this relation is assumed to be a single diffuse reflection, the image formation can be summarized as the convolution of a scatterers map by an ultrasonic field model. This technique has been validated by the simulation of high resolution ultrasound scans of small regions.

Our objective is to propose a fast ultrasound image simulation from preoperative CT volumes. More particularly we wish to simulate abdominal and renal ultrasound scans. For a fast ultrasound image simulation, the model proposed by Bamber and Dickinson [3] seems to be the most appropriate. However, the main statement of this method is that the US pulse and beam shape are assumed invariant. This assumption is only true within small regions and leads to limit the computation of the US images of these small regions. We extended Bamber and Dickinson's model to produce an image from the whole abdomen.

Materials and Methods

The starting data is an image (or a sub-volume) extracted from the 3D CT volume where the pixel (or voxel) size is known. The geometry and the characteristics of the ultrasound probe (circular probe, transducers number and size, US pulse frequency, quality factor Q of the US pulse emission spectrum, etc.) are the input parameters.

Bamber and Dickinson's model: It is based on a linear modeling ² of the properties of an ultrasonic signal reflected diffusely in an inhomogeneous medium. This model which derives from the wave equation, describes the signal as the integration of impulse responses:

¹In 2000, Jensen reports on the results of a fast version of its algorithm. The computation of a 64x64 image simulation with 200,000 scatterers takes more than 3 hours [2].

²Our model is linear because it uses Born's approximation to solve the wave propagation equation in inhomogeneous medium.

$$I_{3D}(x, y, z) = \int \int \int H_{3D}(x, y, z, \alpha, \beta, \gamma) \cdot T(\alpha, \beta, \gamma) \cdot d\alpha \cdot d\beta \cdot d\gamma \quad (1)$$

Where:

- I_{3D} , is the resulting 3D radiofrequency image.
- y is the propagation direction (the axial direction) of the ultrasound wave, x its lateral direction and z its transverse direction.
- H_{3D} , the system impulse response or Point Spread Function (PSF), i.e. the 3D radiofrequency image of a point.
- T , is a function describing the tissue echogenicity. T depends directly on the tissue acoustical impedance.

For a small region, the PSF H_{3D} can be assumed as invariant in space. Equation (1) can so be written as a convolution product:

$$I_{3D}(x, y, z) = H_{3D}(x, y, z) * T(x, y, z) \quad (2)$$

The PSF $H_{3D}(x, y, z)$ is generally modeled as a wave modulated by a Gaussian envelope:

$$H_{3D}(x, y, z) = e^{-\frac{1}{2}(\frac{x^2}{\sigma_{lat}^2} + \frac{y^2}{\sigma_{ax}^2} + \frac{z^2}{\sigma_{trans}^2})} \cos(2\pi fy) \quad (3)$$

Where:

- f is the spatial pulse frequency.
- σ_{ax} is representative to the pulse length and is directly related to the pulse emission spectrum bandwidth.
- σ_{lat} and σ_{trans} are respectively representative to the pulse width and thickness. They are directly related to the transducers geometry and size.

$T(x, y, z)$, the function describing the tissues echogenicity is given by:

$$T(x, y, z) = \frac{1}{2Z_0} \frac{\delta^2}{\delta y^2} (Z_{3D}(x, y, z)) \quad (4)$$

Where Z_0 is the acoustical impedance referential, and $Z_{3D}(x, y, z)$ the tissue acoustical impedance.

The radiofrequency image of a slice (a 2D scan) for a specific $z=const$ can be computed by (dropping $1/2Z_0$ for simplicity):

$$I(x, y) = I_{3D}(x, y, const) = H_{3D}(x, y, const) * \frac{\delta^2}{\delta y^2} (Z_{3D}(x, y, z)) \quad (5)$$

I_B , the final simulated B-scan ultrasound image is obtained by an envelope detection of the radiofrequency image. This detection can be performed by:

$$I_B(x, y) = |I(x, y) + j \cdot Hilbert(I(x, y))| \quad (6)$$

Where $Hilbert()$ is the Hilbert transform.

In their model, Bamber and Dickinson made the assumption of a space invariant PSF. This is true only with parallel wave propagation within small tissue regions.

Bamber and Dickinson's model adaptation to abdominal ultrasound images: Several points have to be taken into account when dealing with abdominal ultrasound: the probe is generally circular and no more linear; the PSF has to be physically adapted to the probe geometry and emission spectrum (it shape depends directly on the propagation direction and on the beam shape which is not constant during the propagation); the high field of view leads also to resolution problems. The adaptation has been performed on the following way:

- (1) Spatial geometry of a circular ultrasound probe. The abdominal ultrasound probes are circular with a different propagation direction for each transducer. However, Bamber's model assumed parallel wave propagation. A Cartesian/polar transform allows recovering a parallel propagation direction. The image formation framework has been adapted as following (Figure 1):

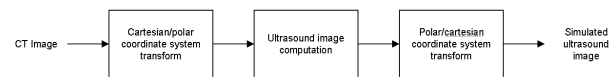


Figure 1: Adaptation to the circular probe geometry

- (2) Image resampling in order to respect Shannon's sampling theorem. The CT image voxel (or pixel) size (around 0.7 mm) is generally greater than the ultrasound wavelength (with a 1540 m/s ultrasound propagation speed in the human tissues and a 3.5 MHz pulse frequency, the wavelength is $\lambda=c/f=0.44$ mm). The PSF H_{3D} is directly related to the wavelength (cf. Equation 3). So, in order to respect Shannon's sampling theorem the transformed CT scan in polar coordinate system has to be resampled by linear interpolation along the propagation axis (see Figure 2-b).
- (3) Macroscopic tissue modeling. Tissues are modeled by their acoustical impedance. A simple threshold based segmentation organizes the CT image into several tissue classes (bone, soft tissues, fat and air). According to the classification, acoustical impedances are allocated to each image pixel. However, the main part of an ultrasound image consists of a speckle pattern. Speckles come from the signal reflected by tissue micro-inhomogeneities (tissues cells, capillaries, blood cells, etc.) which are not directly deducible from the CT data. These micro-inhomogeneities are generally simulated by randomly placed scatterers (see [2] for example). We chose to model them by a thresholded Gaussian noise texture with a magnitude and standard deviation depending on the tissue class (see figure 2-c).
- (4) Probe geometrical and spectral influence on the PSF; adaptive spatial PSF modeling. The probe spectrum and the transducers geometry allow defining directly the PSF. σ_{ax} is deduced directly from the pulse emission spectrum quality factor Q and the wavelength λ :

$$\sigma_{ax} = \frac{\lambda \cdot Q \cdot \sqrt{\ln(2)}}{\pi} \quad (7)$$

The constant ultrasonic field assumption is no more verified. The ultrasonic field spatial variation is modeled by the PSF spatial variation. The beam expansion has been simulated as following:

$$\begin{aligned} \sigma_{lat}(y) &= \sigma_{lat}(0) + k_1 \cdot y \\ \sigma_{trans}(y) &= \sigma_{trans}(0) + k_2 \cdot y \end{aligned} \quad (8)$$

$\sigma_{lat}(0)$ and $\sigma_{trans}(0)$ are deduced directly from the transducer geometry (the Gaussian Full Width Half Maximum FWHM of $\sigma_{lat}(0)$ and $\sigma_{trans}(0)$ has been set respectively to the width and height of the transducer) and k_1 and k_2 from the ultrasound propagation physics. The PSF is also described within the polar coordinate system. This transform also depends on its spatial location.

Results

The previous methodology has been evaluated on a slice extracted from an abdominal CT volume. The objective of this study is a kidney ultrasound image simulation with the classical probes used by urologists.

Methodology implementation: In a first study we choose to simulate an image produced by a classical C2 5 circular ultrasound scanning probe. The simulated probe is a 128 transducers curved array with a curvature radius of 40mm that geometrically steers to a maximum sector angle of 60 degrees. The simulated pulse frequency is 3.5 MHz with a Q quality factor of 10 ($\sigma_{ax} \approx 3 \cdot \lambda$). The image depth has been set to 22 cm from the probe.

The CT scan volume extracted slice is a 512x512 image with a pixel size of 0.68 mm.

The tissue acoustical impedances of the several organs have been found in the literature. They have been set to 1.35, 1.25 and 5 kg/m²/s for respectively fat, soft tissues and bone.

The figure 2 presents the several steps of the ultrasound image simulation processing:

a) The starting CT scan image. The beam position and the simulated ultrasound image final geometry have been enhanced.

b) The image in polar coordinate system. After the coordinate system transform, the image has been resampled along the propagation direction in order to respect Shannon's sampling theorem. For f=3.5 MHz ($\lambda=0.44$ mm) and a 0.68 mm pixel size, an interpolation ratio of 4 has been chosen.

c) Acoustical impedance map. This map is obtained after segmentation of the previous image in several classes (bone, soft tissues, water and fat). The tissue acoustical impedances have then been modulated by a noise texture in order to model the micro-inhomogeneities (the impedances are represented as gray level on the Figure).

d) Resulting radiofrequency image. It has been obtained after convolution of the PSF H_{3D} with the second order derivate along the propagation axis of the acoustical impedance map. The radiofrequency image has been normalized on the Figure.

e) Radiofrequency image envelop detection. The radiofrequency image is considered as the envelop real part, its imaginary part is estimated using the Hilbert Transform. The final image is the magnitude of this complex.

f) Final simulated ultrasound image after back transformation in Cartesian coordinate system. The final has a size of 1200x1200. The computing time of this image is less than 5 seconds on a classical PC (AMD Athlon 2200+, 1Mo RAM).

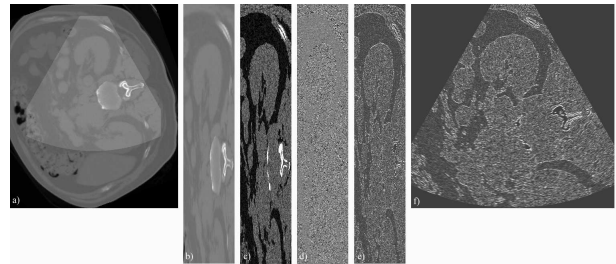


Figure 2: Ultrasound image simulation: a) CT image; b) polar transformation and resampling; c) acoustical impedance map; d) radiofrequency image after convolution of acoustical impedance map with the PSF; e) radiofrequency image envelop detection calculated with the Hilbert transform; f) simulated ultrasound image after polar/Cartesian transformation.

Pulse frequency influence: The pulse frequency influence can be seen on the next two images. One image has been simulated with a f=1 MHz, the other with f=5 MHz (figure 3). The influence of the pulse frequency on the spatial resolution is easily perceptible on the images. In these images we did not care on the signal attenuation caused by tissues absorption (cf. discussion).

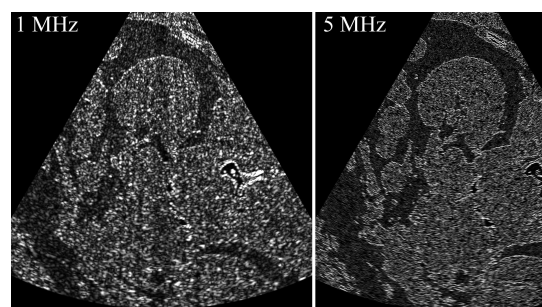


Figure 3: Ultrasound image simulations with f=1 MHz (left) and f=5 MHz (right).

Probe influence: On figure 4, two images have been produced by the simulation of two probes having the same size and pulse frequency but one with 128 transducers and the other with 64 transducers. The number of elements and their size have a direct impact on the lateral

resolution of the simulated images.

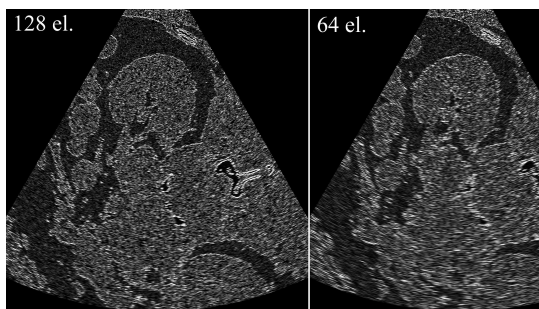


Figure 4: 3.5MHz Ultrasound image simulations with a 128 (left) and a 64 elements probe (right).

Real and simulated ultrasound images comparison:

We wished to compare qualitatively a real kidney ultrasound image found in the literature with a simulated one. In both cases the pulse frequency was 3.5 MHz (figure 5). Because the observed scene is different between the two images, the only ambition of this comparison is to present the mutual characteristics of both images but also the disparities between our model and a real ultrasound image.

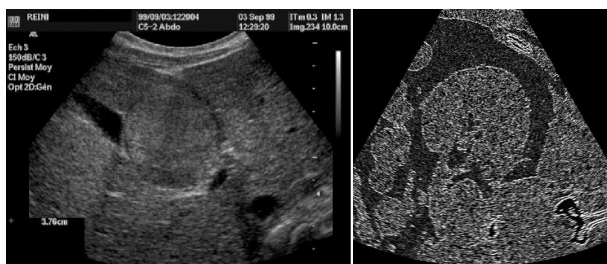


Figure 5: Comparison between a real 3.5MHz ultrasound image (left) and a simulated one (right).

Discussion

Qualitatively, we find in the simulated ultrasound image some of the main characteristics of a real ultrasound image:

- The simulated ultrasound image is mainly produced by speckle patterns which are organized on concentric circles. The speckle size grows when the distance to the probe increases.
- The pulse frequency and the number of probe transducers seem to have the expected behavior on the simulation. Higher pulse frequencies give finer speckle in the axial direction and so enhance the spatial image resolution. A high number of transducers provides finer speckle in the lateral direction.
- The acoustical interface between tissues is well delineated.

However, other ultrasound image characteristics have not been taken into account. This is the case for example

of the signal attenuation by the medium absorption. Ultrasound devices compensate this attenuation by amplification with a gain increasing with the depth. This gain has the effect to enhance the attenuated signal but also the noise. In our simulation, this gain could simply modeled by a Gaussian noise with a magnitude and a standard deviation increasing exponentially with the distance to the probe.

Other ultrasound image characteristics like acoustic shadow or mirror effect are totally absent on the simulated images. This lack comes directly from the used model where the wave propagation and reflection are not simulated explicitly; however, these effects are generally considered as artifacts on the real ultrasound images.

But beyond these remarks, additional differences between simulated and real images remain. Firstly we have not taken the operators pressure on the probe and the resulting organs deformation into account. Secondly, a great aspect difference is provided by our tissue micro-inhomogeneities model. Seeing that the main aspect of an ultrasound image is provided by the speckle, a more realistic modeling of tissue inhomogeneities should enhance the realism of the simulated image.

The simulation computer time is short in comparison to other simulation approaches (a few seconds on a classical PC). However this time still remains to long for a real time simulation.

Conclusions

This study presents the first results of an abdominal ultrasound image simulation. The model proposed by Bamber and Dickinson has been efficiently adapted to a high field of view ultrasound image simulation obtained by a circular probe. These simulations have been obtained in a fairly fast computation speed and qualitatively they present most of the real ultrasound images main characteristics: influence of the transducers number and US frequency, speckle position and shape, acoustical interface between tissues... In the future, a more accurate tissue inhomogeneities model should enhance the simulation quality. A more formal evaluation is also under process.

References

[1] J. A. JENSEN. Field: a program for simulating ultrasound systems. *Med Biol Eng Comput*, 34:351–353, 1996.

[2] J. A. JENSEN and S. I. NIKOLOV. Fast simulation of ultrasound images. *Proc. of IEEE Int. ultrasonic Symp., Puerto Rico*, pages 1721–1724, 2000.

[3] J. C. BAMBER and R. J. DICKINSON. Ultrasonic b-scanning: a computer simulation. *Phys Med Biol*, 25:463–479, 1980.